SO_2 AND NO_2 SIMULATION AND VALIDATION IN METROPOLITAN LIMA USING WRF-CHEM MODEL

ANA LUNA[1], HECTOR NAVARRO[1,2] & ALDO MOYA[3]
[1] Universidad del Pacífico (Lima, Perú).
[2] Facultad de Ciencias Físicas, Unidad de Posgrado, Universidad Nacional Mayor de San Marcos (Lima, Perú).
[3] Instituto Geofísico del Perú (Lima, Perú).

ABSTRACT

In recent times, air pollution in Peru is attracting the attention of the population and the government as well, who finally makes the policies that help us to preserve good air quality. In this research, we used the chemical-meteorological model Weather Research and Forecasting coupled with Chemical (WRF-Chem v3.8) to predict pollution scenarios. We studied and analyzed three 2017 months of summer (January, February and March) and three months of winter (July, August and September) to evaluate and forecast two pollutants concentration, sulfur dioxide (SO_2) and nitrogen dioxide (NO_2) over the city of Lima. We also considered the meteorological variables such as the wind speed and its direction, average temperature, relative humidity and atmospheric pressure. Besides, we used fixed industrial sources inventory as emission data and the Global Forecast System (GFS) as border data for the meteorological components. Within the WRF-Chem model, we implemented the Grell-Freitas parameterization of convection to represent the clouds; we used RRTMG for the shortwave/longwave radiation scheme, and the Monin-Obukhov for the processes in the surface layer, among others. On the other hand, for the gas phase chemistry, we used the RADM2 scheme, for the aerosol module we utilized the MADE-SORGAM, and finally, we employed the Fast-j photolysis scheme. We finally compared the results with the data provided by the ten monitoring stations that belong to the National Service of Meteorology and Hydrology (SENAMHI) which are located in strategic zones in Lima.

Lastly, we showed that the variables studied are within the environmental quality standard authorized by the Ministry of the Environment, and we also demonstrated that the simulations given by the model are, in general, overlapping the values measured experimentally in all of the monitoring stations evaluated.

Keywords: Air pollution, Forecasting, Industrial emissions, WRF-Chem.

1 INTRODUCTION

In the last decades, several researchers have published the correlation between the decrease in the quality of life and the increase of allergies and respiratory and cardiovascular diseases with air pollution, in particular, with the high levels of industrial and vehicular emissions [1–3].

In more populated areas, industrial activities become more dangerous [4], and have a significant impact not only on ecology and agriculture but also on health. Particles that are in the atmosphere are relatively large sediment, and due to the turbulence in the air, they cannot be maintained in suspension for an extended period. On the other hand, smaller particles can be transported for long distances, so their impact can reach cities far from the source of emission, while they can interact with other air pollutants and cause severe damage [5–8].

Due to this problem, the scientific community began to develop research aimed at determining the chemical composition of atmospheric pollutants, at understanding how they are distributed, and which regions are most predominant, to allow preventive and corrective decisions to take to safeguard the health. One of these is the experiment carried out in China to characterize some factors that control the dispersion of air pollutants in the city of Shanghai, confirming the importance of the direction and the wind speed in the distribution of the aerosols [9].

ISSN: 2046-0546 (paper format), ISSN: 2046-0554 (online), http://www.witpress.com/journals
DOI: 10.2495/CMEM-V8-N2-135-147

The pollutants distribution's evaluation in a city can be analyzed and studied through monitoring networks or using the so-called dispersion models. The town of Lima has several air quality monitoring stations, belonging to the Directorate-General for Environment Quality of the Vice Ministry of the Environmental Management, which depends on the Ministry of the Environment (MINAM). In these stations, pollutant measurements are recorded, such as NO_x, SO_2, $PM_{2.5}$, PM_{10}, O_3, and CO. One of the most commonly used predictive models with chemical coupling in the last decades is the WRF-Chem, which has a modular structure that contemplates meteorological and chemical processes simultaneously, considering the effects on the radiation balance, and the interaction of the aerosols with clouds through the nucleation of the drops [10–12].

In recent years, several articles were published in which the model mentioned above, was used to different cities [13–18]. In the particular case of Peru, the authors of Ref. [19] carried out a study on the dispersion of PM_{10} particles in the air, produced by burning biomass, with the help of that model.

Taking into account that the city of Lima is characterized by almost the total absence of rainfall, high relative humidity, and a persistent cloud cover; the primary objective of this work is to evaluate the impact of industrial sources of pollution on that city, using the WRF-Chem model.

2 DATA AND METHODOLOGY

In this section, we detail the software employed, how the configuration of the model was carried out, and the description of the data used.

2.1 WRF-Chem description

The Weather Research and Forecasting coupled with Chemical (WRF-Chem), is a regional model developed in the NOAA (National Oceanic and Atmospheric Administration) [10], which is used to simulate and predict the dispersion and concentration of atmospheric pollutants; it has multiple physical and chemical settings. The WRF-Chem solves Eulerian type equations with its Advanced Research WRF (ARW) core for this purpose. Their codes are free and are continually being improved by both, their developers and the user community around the world. For this research, we used v3.8 of the WRF-Chem.

2.1.1 Model Configuration

For the simulation, we evaluated the first week of six different months: January, February, March, July, August, and September of 2017. The first three months comprise the summer season and the rest of the months belong to the coldest season, winter, for Lima-Peru. To evaluate the pollutant levels, we took a single domain of 4x4 *km* which covers approximately 169.744 km^2 (Fig. 1). Within this region, the pollutants sulfur dioxide (SO_2) and nitrogen oxides (NO_x) were coupled. The details of the domain configuration and boundary conditions are in Table 1, and the meteorological, physical and chemical parameterizations used are summarized in Table 2.

For parameterization of short and longwave radiation, we used the Rapid Radiative Transfer Model for General Circulation Models (RRTMG), which aims to estimate the radiative flows and cooling speeds more accurately. This scheme uses the k-correlation approximation method for the calculation of radiation, which allows greater precision and computational efficiency. For the surface layer, we employed the Monin-Obukhov scheme, based on the

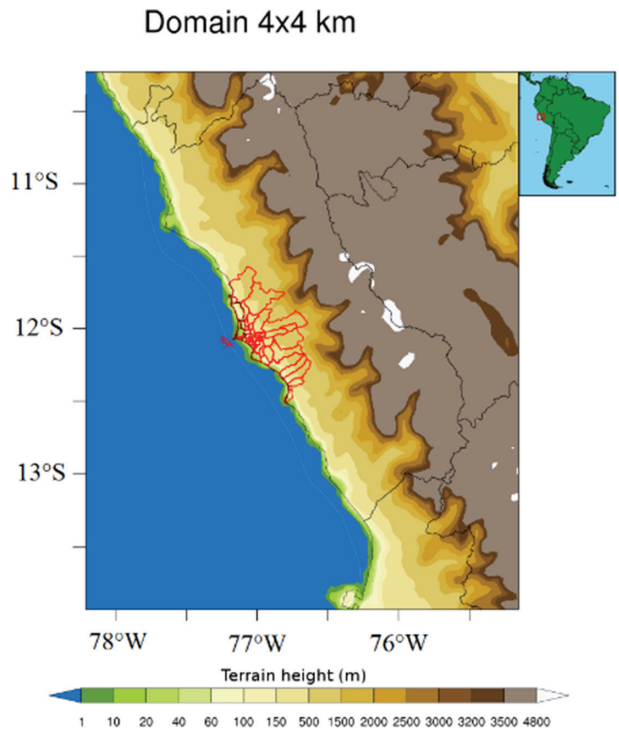

Figure 1: Simulation domain. Lima-Peru.

relationship between the diffusion coefficients and the turbulent kinetic energy. On the other hand, the land surface was parameterized with the Noah scheme, which contemplates various physical processes, as the evaporation of water directly from the soil, or from the surfaces with water, the evapotranspiration of the vegetation and the heat flow with the ground and the plant surface (Turbulent Heat Flux), which are essential processes in water balance studies. In the case of the planetary boundary layer, we used the ACM2 scheme [20], which includes a first-order Eddy diffusion component, in addition to the explicit non-local transport of the original ACM1 scheme. This modification allows for improving the shape of vertical profiles

Table 1: Characteristics of the domain and the contour conditions used.

Grid size	4 km
Domain center	(−12.083796 , −77.048449)
Number of points in x	105
Number of points in y	105
Number of points in z	30
Geographical data	30 arc seconds
Meteorological fields	GFS 0:25 every 3hrs.
Simulation period	7 days

Table 2: Physical and chemical parameterizations.

Atmospheric process	**WRF-Chem option**
Long wave radiation	RRTMG
Shortwave radiation	RRTMG
Surface layer	Monin-Obukhov
Earth surface	Noah
Planetary boundary layer	ACM2
Cumulus	Grell-Freitas
Microphysics	Lin (Purdue)
Chemistry of the gas phase	RADM2
Aerosol module	MADE-SORGAM
Photolysis	Fast-J

near the surface. On the other hand, to model the clouds, we chose the Grell-Freitas (GF) convection parameterization, in which the mass flow of the cloud base varies quadratically as a function of the convective updraft fraction in the global model hydrostatic [21]. For the cloud microphysics, we employed the sophisticated Purdue-Lin scheme which was designed as a one-moment water mass conserved microphysics scheme with five hydrometeors: cloud water, rain, cloud ice, snow and graupel ([22]; [23]).

Regarding the configuration of the chemistry of the model, we used the regional model of acid deposition for the gases, version 2 (RADM2). The inorganic species included in the RADM2 mechanism are 14 stable species, four reactive intermediates and three abundant stable species (oxygen, nitrogen, and water). The aerosol module used is based on the Modal Aerosol Dynamics model for Europe (MADE) [24], which incorporates secondary organic aerosols (SORGAM). MADE – SORGAM contemplates simultaneously aerosol nucleation, condensation, and coagulation. It considers the classical modal description of the atmospheric aerosol diametric distribution through three continuous distributions of the log-normal type (Aitken, accumulation and coarse modes, corresponding approximately to the PM_{10}-$PM_{2.5}$ range). Finally, the Fast-J photolysis scheme was used, which calculates the photolysis rates in the presence of an arbitrary mixture of cloud layers and aerosols. The algorithm is fast enough to allow the scheme to be incorporated into 3-D global chemical transport models and to have photolysis rates updated every hour [25].

2.2 Data description

In this current work, we used three types of data, those that make up the initial and contour conditions of the model, the data related to the chemical species under study and the inventory of concentrations to execute the verification of the results of the model.

2.3 Initial data and boundary conditions

The data produced by the Global Forecast System (GFS) model, developed and administered by the National Oceanic and Atmospheric Administration (NOAA), of the United States of America, are used. The data contain information on atmospheric pressure at sea level,

Table 3: Locations of the air quality monitoring stations.

Station Name	Latitude	Longitude
Ate (ATE)	−12.0261	−76.9186
Santa Anita (STA)	−12.043	−76.9714
San Juan de Lurigancho (SJL)	−12.0169	−76.9988
Carabayllo (CRB)	−11.9022	−77.0336
Puente Piedra (PPD)	−11.8632	−77.0741
San Martn de Porres (SMP)	−12.0089	−77.0845
Campo de Marte (CDM)	−12.0705	−77.0432
San Borja (SBJ)	−12.1086	−77.0078
Huachipa (HCH)	−12.0169	−76.9488
Villa Maria del Triunfo (VMT)	−12.1664	−76.9200

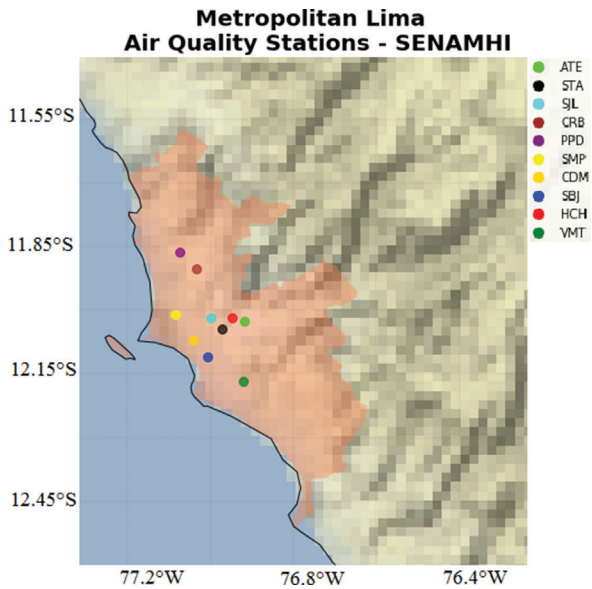

Figure 2: The different coloured dots represent the locations of the air quality monitoring stations.

temperature, humidity, speed and wind direction on the surface and different levels of the troposphere; and the geopotential height. They are available in https://rda.ucar.edu/datasets/ds084.1/index.html#sfol-wl-/data/ds084.1?g=20170101

2.3.1 Emission Data

The emission data are the basis for the model to reproduce pollution scenarios. In this case, we took this information from the Lima emissions inventory, provided by the General Directorate of Environmental Health (DIGESA, 2005). The data were prepared using the

methodology of Economopoulos *et al*. [26]. We used emissions from 75 industries located in different areas of the city. Among the variables used were sulfur dioxide (SO_2) and nitrogen dioxide (NO_2).

2.3.2 Validation Data

We used the data from the monitoring network of the National Service of Meteorology and Hydrology of Peru (SENAMHI) for the verification process and the validation of the simulation's results. SENAMHI has ten monitoring stations for air quality in Metropolitan Lima, whose location details are in Table 3 and Fig. 2. The primary atmospheric pollutants taken into consideration were nitrogen dioxide (NO_2) and sulphur dioxide (SO_2).

3 INDICATORS FOR EVALUATING THE OBTAINED FORECASTING

We used Pearson correlation coefficient (r), the index of agreement (IOA) and the mean absolute error (MAE). The first one indicates how strong is the linear relationship between the output data set of the model and the observation data. On the other hand, the IOA is a standardized measure of the degree of model prediction error, and finally, the MAE quantifies the average absolute magnitude of the errors.

4 RESULTS

4.1 Meteorology

The meteorology has a high impact on the formation, transport, emission and deposition of atmospheric pollutants [27]; that is why we studied and analyzed the meteorological variables temperature and wind (direction and speed). Figure 3 shows three images with the temperature average and the direction and speed of the wind at 10 meters from the surface, these maps correspond to the summer months, and they show an increase in temperature from January to March. During this period, the maximum temperature reached values were 30.6, 30.9 and 31.6°C for January, February and March, respectively. Regarding the wind speed, the average values reached were 6.2, 6.5 and 5.8 m/s, which according to the Beaufort scale is a moderate wind, with a predominant direction from south to north in the coastal area.

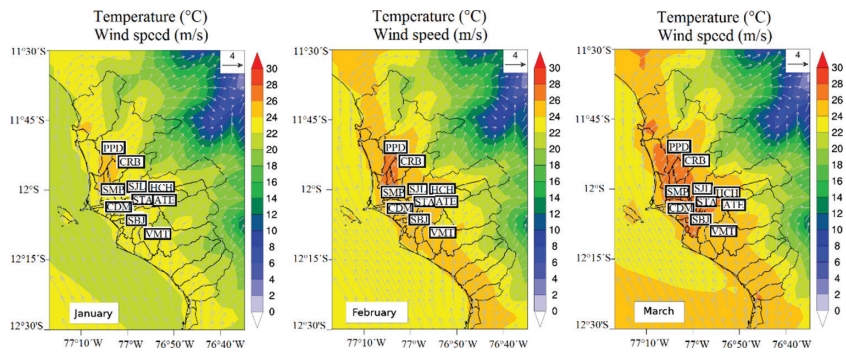

Figure 3: Average values of temperature, speed and wind direction for the summer months studied; (a) January, (b) February and (c) March.

Figure 4 is analogous to Fig. 3 but for the winter season. The maximum temperatures were 25.3, 22.3 and 22.8°*C*, and the average wind speeds were 6, 4.9 and 5.1 *m/s* (moderate wind, according to the Beaufort scale) for July, August and September, respectively. The trend of the direction of the wind is the same as in the summer season; winds go from south to north. The color palette at the right side of each image indicates the intensity of the temperature in the studied area, and the arrows represent the direction and intensity of the wind.

4.2 Chemical variables

4.2.1 Sulfur dioxide (SO_2)

Figure 5 shows three images that correspond to the average of SO_2 for the summer months. There is an increase of SO_2 as the temperature increases; this could have a relationship with the photolysis reactions that occur in the presence of the sun's rays. We also showed the direction of the wind represented by the vectors (arrows) which indicate the predominance of the wind from south to north, the same tendency has the pollutant, especially during March (a small plume with the same direction of the wind is observed).

Figure 6 shows the dispersion of SO_2 during the winter period, in which the concentrations are even lower than during the summer season. The SO_2 highest levels were obtained in the

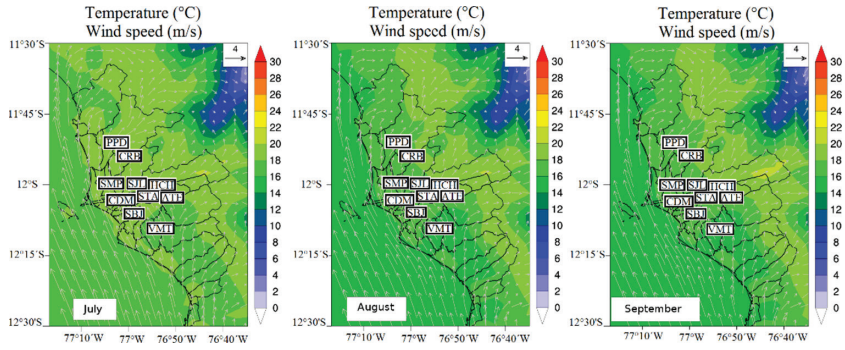

Figure 4: Average temperature and wind (direction and intensity) for the winter months studied; (a) July, (b) August and (c) September.

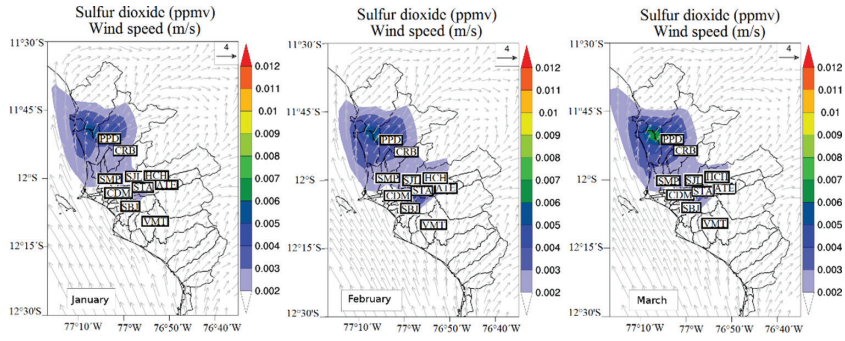

Figure 5: The monthly SO_2 average concentration for (a) January, (b) February and (c) March.

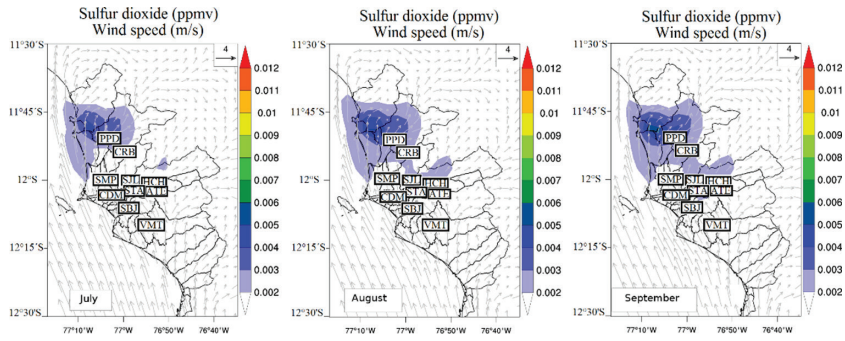

Figure 6: The monthly average concentration of sulfur dioxide (SO2) for the study period; (a) July, (b) August and (c) September.

vicinity of the emission sources; the same tendency could be seen in Fig. 5. In both figures, the colour palette indicates the amount of SO_2 in parts per million volume (ppmv) and the arrows indicate the direction and intensity of the wind.

Figure 7 shows the SO_2 time series for the whole study period correspondent to the SENAMHI Puente Piedra (PPD) monitoring station, at the north of Metropolitan Lima. The blue line represents the measured data, and the red line is the data modelled with the WRF-Chem. There is a high correspondence between both of them. However, in the first month, the model overestimates the concentration levels of SO_2, this fact could be related to the required spin-up time for the model.

4.2.2 Nitrogen dioxide (NO_2)

As the *SO2* pollutant, the NO_2 is also sensitive to the temperature values (Fig. 8), so we inferred that the photolysis contributes to increasing the concentration of this pollutant. As a result, NO_2 levels go up as the summer months pass, and even in March, we observed an orange spot. The action of the wind in the dispersion of NO_2 is also clearly displayed in the image since the plume has the orientation from south to north, just like the arrows.

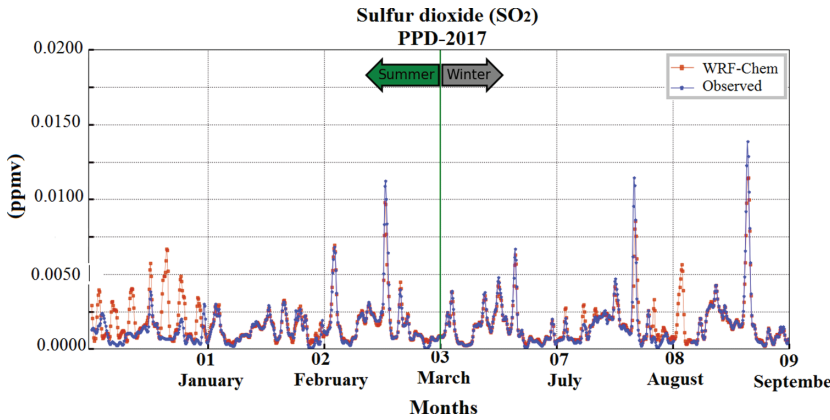

Figure 7: Six months' time series studied for PPD station, located at the north of Metropolitan Lima.

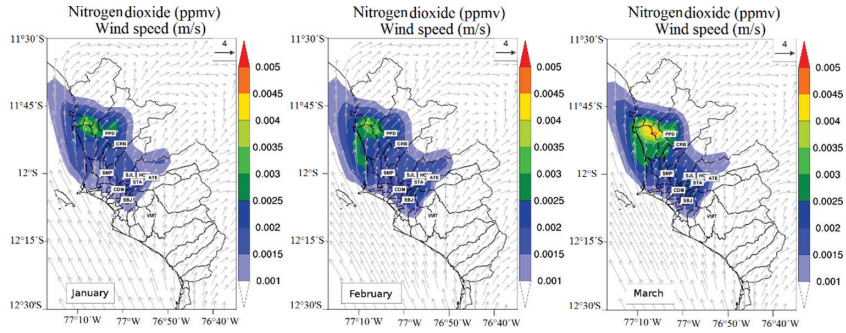

Figure 8: The monthly average concentration of NO_2 for the study period; (a) January, (b) February and (c) March.

Figure 9 shows the distribution of NO_2 over the study area, for the months of the winter season July, August and September.

Figure 10 represents the time series of the concentrations of NO_2 at the PPD station at the north of Metropolitan Lima. The blue line shows the observed data by the SENAMHI monitoring station, and the red line indicates the modelling with the WRF-Chem. A high correlation is observed between both, the measured and the simulated data.

4.2.3 Metrics

The three metrics calculated of the two studied pollutants for the summer and winter periods are presented in Table 4 (a) (b).

In the case of the SO_2 pollutant, Table 4(a) shows the correlations and acceptance indices which are far from those expected during the summer period, except for the VMT station. During the winter period, the VMT station was again the one that obtained the best values of statistical metrics. On the other hand, the station whose results deviated most from the expected values was CRB.

We observed in the Table 4(b), corresponding to the pollutant NO_2, that during the winter months there were two monitoring stations, SJL and VMT, for which the amount of data are not sufficient to validate the predictions thrown by the model.

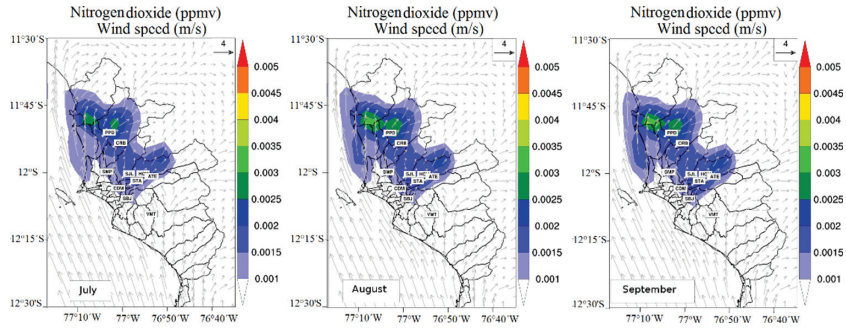

Figure 9: The monthly average concentration of NO_2 for the study period; (a) July, (b) August and (c) September.

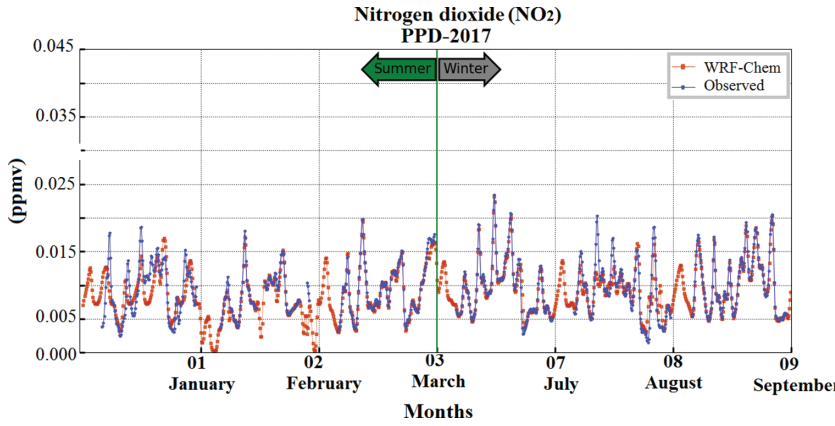

Figure 10: Six months' time series studied for PPD station, located at the north of Metropolitan Lima.

During the summer season, the best results of the metrics were obtained for the VMT station; while the one with the worst parameters is the ATE station. Regarding the winter period, the HCH station shows an IOA of 0.985 and the best r (0.975), indicating that there is a close correspondence between the predicted or simulated value and the value observed in that period; in addition to a high linear correlation between the modeled value and the observed value, respectively.

5 CONCLUSIONS

The chemistry–meteorological model WRF-Chem, version 3.8, was implemented to reproduce pollution scenarios during 2017 with emission data corresponding to fixed sources of the city of Metropolitan Lima and meteorological border data that belong to the GFS. We used a 4 km domain with a centre in the city of Metropolitan Lima.

The temperature and wind meteorological variables were adequately modelled and represented by the WRF-Chem, both for the summer and winter periods. For the pollutant SO_2, we observed high levels during the summer period and moderate ones in winter. On the other hand, none of the 10 SENAMHI monitoring stations registered values that exceeded the quality standard proposed by MINAM. For the pollutant NO_2, we obtained the same tendency; high values were collected in the summer months and moderate amounts in the winter season. In this case, the quality standard was not exceeded either. We inferred that the concentrations of both pollutants, the SO_2 and the NO_2, are not only emitted by the fixed sources but are also increased by the action of photolysis. Pollution stains shown on the heat maps for both pollutants were located in the areas where there is the most significant number of factories (Callao, Puente Piedra and ATE), coinciding with the location of the emission sources used in this study.

The metrics studied strengthen, in general, the results modelled with the WRF-Chem.

Table 4: Values obtained for the indicators studied corresponding to SO_2 (a) and NO_2 (b). The best results have been highlighted in bold and the values that deviate most from the desired values were written in italics.

	(a)						(b)					
Pollutant	***SO_2*: Jan.–Feb. –Mar.**			***SO_2*: Jul.–Aug.–Sept.**			***NO_2*: Jan.–Feb. –Mar.**			***NO_2*: Jul.–Aug.–Sept.**		
Metrics & Stations	MAE	IOA	r	MAE	IOA	r	MAE	IOA	r	MAE	IOA	r
ATE	*0.0012*	0.735	0.532	0.00045	0.970	0.946	*0.0022*	*0.851*	*0.756*	*0.0020*	0.928	0.883
STA	0.00019	0.873	0.745	0.0002	0.960	0.946	0.00096	0.967	0.940	0.00069	0.980	0.965
CDM	0.00023	0.778	0.560	0.00011	0.957	0.936	0.00049	0.965	0.932	0.0010	*0.855*	*0.744*
SMP	0.00055	*0.498*	**0**.*323*	0.00012	0.966	0.935	0.00059	0. 927	0.865	**0.0004**	**0.985**	0.974
SBJ	0.00020	0.941	0.887	0.00011	0.969	0.944	0.00053	0.965	0.938	0.00047	0.960	0.925
PPD	0.0006	0.834	0.709	0.00031	0.937	0.887	0.0014	0.890	0.795	0.0010	0.951	0.912
CRB	0.00026	0.896	0.711	*0.00065*	*0.684*	*0.464*	0.00075	0.966	0.936	0.00079	0.968	0.947
HCH	0.00035	0.903	0.819	0.00020	0.986	0.975	0.0014	0.918	0.855	0.00071	**0.985**	**0.975**
SJL	0.00033	0.851	0.740	0.00023	0.963	0.942	0.00094	0.968	0.941	-	-	-
VMT	**0.00011**	**0.951**	**0.911**	**0.000063**	**0.996**	**0.993**	**0.00032**	**0.980**	**0.964**	-	-	-

REFERENCES

[1] Hung, L.J., Chan, T.F., Wu, C.H., Chiu H.F. & Yang, C.Y., Traffic air pollution and risk of death from ovarian cancer in Taiwan: Fine particulate matter ($PM_{2.5}$) as a proxy marker. *Journal of Toxicology and Environmental Health*, *Part A*, **75(3)**, pp. 174–182, 2012. https://doi.org/10.1080/15287394.2012.641200

[2] Landrigan, P.J., Air pollution and health. *The Lancet Public Health*, **2(1)**, pp. e4–e5, 2017. https://doi.org/10.1016/s2468-2667(16)30023-8

[3] Womg, G.W.K., Air pollution and health. *The Lancet Respiratory Medicine*, **2(1)**, pp. 8–9, 2014. https://doi.org/10.1016/s2213-2600(13)70284-4

[4] Matejicek, L., Spatial modelling of air pollution in urban areas with GIS: A case study on integrated database development. *Advances in Geosciences*, **4**, pp. 63–68, 2005. https://doi.org/10.5194/adgeo-4-63-2005

[5] World Health Organization. *Air Quality Guidelines: Global Update 2005: Particulate Matter, Ozone, Nitrogen dioxide, and Sulfur dioxide*. 2006.

[6] Hashim, B.M., *Measurement and Study Concentrations Some Air Pollutants in Baghdad City*. Thesis Doctoral. M Sc thesis College of Science Al-Mustansiriyah University. 2009.

[7] Al-Saadi, G.M., Assessment of air and water pollution due to operation south of Baghdad power plant. *Building and Construction Engineering Department*, University of Technology, p. 147, 2012.

[8] Leili, M., Naddafi, K., Nabizadeh, R., Yunesian, M. & Mesdaghinia, A., The study of TSP and PM_{10} concentration and their heavy metal content in central area of Tehran, Iran. *Air Quality, Atmosphere & Health*, **1(3)**, pp. 159–166, 2008. https://doi.org/10.1007/s11869-008-0021-z

[9] Tie, X., Geng, F., Guenther, A., Cao, J., Greenberg, J., Zhang, R. & Cai, C., Megacity impacts on regional ozone formation: observations and WRF-Chem modeling for the Mirage-Shanghai field campaign. *Atmospheric Chemistry and Physics*, **13(11)**, pp. 5655–5669, 2013. https://doi.org/10.5194/acp-13-5655-2013

[10] Grell, G.A., Peckham, S.E., Schmitz, R., McKeen, S.A., Frost, G., Skamarock, W.C. & Eder, B., Fully coupled online chemistry within the WRF model. *Atmospheric Environment*, **39(37)**, pp. 6957–6975, 2005. https://doi.org/10.1016/j.atmosenv.2005.04.027

[11] Fast, J.D., Gustafson Jr, W.I., Easter, R.C., Zaveri, R.A., Barnard, J.C., Chapman, E.G. & Peckham, S.E., Evolution of ozone, particulates, and aerosol direct radiative forcing in the vicinity of Houston using a fully coupled meteorology-chemistry-aerosol model. *Journal of Geophysical Research: Atmospheres*, **111(D21)**, 2006. https://doi.org/10.1029/2005jd006721

[12] Chapman, E.G., Gustafson Jr, W.I., Easter, R.C., Barnard, J.C., Ghan, S.J., Pekour, M.S. & Fast, J.D., Coupling aerosol-cloud-radiative processes in the WRF-Chem model: Investigating the radiative impact of elevated point sources. *Atmospheric Chemistry and Physics*, **9(3)**, pp. 945–964, 2009. https://doi.org/10.5194/acp-9-945-2009

[13] He, H., Tie, X., Zhang, Q., Liu, X., Gao, Q., Li, X. & Gao, Y., Analysis of the causes of heavy aerosol pollution in Beijing, China: A case study with the WRF-Chem model. *Particuology*, **20**, pp. 32–40, 2015. https://doi.org/10.1016/j.partic.2014.06.004

[14] Lowe, D., Archer-Nicholls, S., Morgan, W., Allan, J., Utembe, S., Ouyang, B. & Percival, C., WRF-Chem model predictions of the regional impacts of N_2O_5 heterogeneous processes on night-time chemistry over north-western Europe. *Atmospheric Chemistry Physics*, **15(3)**, pp. 1385–1409, 2015. https://doi.org/10.5194/acp-15-1385-2015

[15] Vara-Vela, A., Andrade, M.F., Kumar, P., Ynoue, R.Y. & Munoz, A.G., Impact of vehicular emissions on the formation of fine particles in the Sao Paulo Metropolitan Area: A numerical study with the WRF-Chem model. *Atmospheric Chemistry and Physics*, **16(2)**, pp. 777–797, 2016. https://doi.org/10.5194/acp-16-777-2016

[16] Abou Rafee, S.A., Martins, L.D., Kawashima, A.B., Almeida, D.S., Morais, M.V., Souza, R.V. & Freitas, E.D., Contributions of mobile, stationary and biogenic sources to air pollution in the Amazon rainforest: A numerical study with the WRF-Chem model. *Atmospheric Chemistry and Physics*, **17(12)**, pp. 7977–7995, 2017. https://doi.org/10.5194/acp-17-7977-2017

[17] Rizza, U., Barnaba, F., Miglietta, M.M., Mangia, C., Di Liberto, L., Dionisi, D. & Gobbi, G.P., WRF-Chem model simulations of a dust outbreak over the central Mediterranean and comparison with multi-sensor desert dust observations. *Atmospheric Chemistry and Physics*, **17(1)**, pp. 93–115, 2017. https://doi.org/10.5194/acp-17-93-2017

[18] Werner, M., Kryza, M., Geels, C., Ellermann, T. & Skjøth, C., Ammonia concentrations over Europe–application of the WRF-Chem model supported with dynamic emission. *Polish Journal of Environmental Studies*, **26(3)**, pp. 1323–1341, 2017. https://doi.org/10.15244/pjoes/67340

[19] Álvarez, M., Saturnino, A., Arredondo, R.E., Posadas, Y. & Ángel, R., Determinación de la presencia de partículas (PM_{10}) en Perú producidas por quema de biomasa con ayuda de modelos numéricos. *Revista internacional de contaminación ambiental*, **33(1)**, pp. 99–108, 2017. https://doi.org/10.20937/rica.2017.33.01.09

[20] Pleim, J.E., A combined local and nonlocal closure model for the atmospheric boundary layer. Part I: Model description and testing. *Journal of Applied Meteorology and Climatology*, **46(9)**, pp. 1383–1395, 2007. https://doi.org/10.1175/jam2539.1

[21] Fowler, L.D., Skamarock, W.C., Grell, G.A., Freitas, S.R. & Duda, M.G., Analyzing the Grell–Freitas convection scheme from hydrostatic to nonhydrostatic scales within a global model. *Monthly Weather Review*, **144(6)**, pp. 2285–2306, 2016. https://doi.org/10.1175/mwr-d-15-0311.1

[22] Lin, Y.L., Farley, R.D. & Orville, H.D., Bulk parameterization of the snow field in a cloud model. *Journal of Climate and Applied Meteorology*, **22(6)**, pp. 1065–1092, 1983. https://doi.org/10.1175/1520-0450(1983)022<1065:bpotsf>2.0.co;2

[23] Chen, S.H. & Sun, W.Y., A one-dimensional time dependent cloud model. *Journal of the Meteorological Society of Japan. Ser. II*, **80(1)**, pp. 99–118, 2002. https://doi.org/10.2151/jmsj.80.99

[24] Ackermann, I.J., Hass, H., Memmesheimer, M., Ebel, A., Binkowski, F.S. & Shankar, U.M.A., Modal aerosol dynamics model for Europe: Development and first applications. *Atmospheric Environment*, **32(17)**, pp. 2981–2999, 1998. https://doi.org/10.1016/s1352-2310(98)00006-5

[25] Wild, O. & Prather, M.J., Excitation of the primary tropospheric chemical mode in a global three-dimensional model. *Journal of Geophysical Research: Atmospheres*, **105(D20)**, pp. 24647–24660, 2000. https://doi.org/10.1029/2000jd900399

[26] Economopoulos, A.P. & World Health Organization., *Assessment of Sources of Air, Water, and Land Pollution: A Guide to Rapid Source Inventory Techniques and their Use in Formulating Environmental Control Strategies*, Geneva: World Health Organization, 1993.

[27] Zhang, H., Wang, Y., Hu, J., Ying, Q. & Hu, X.M., Relationships between meteorological parameters and criteria air pollutants in three megacities in china. *Environmental Research*, **140**, pp. 242–254, 2015. https://doi.org/10.1016/j.envres.2015.04.004